Eur. Phys. J. D **43**, 189–192 (2007)
DOI: 10.1140/epjd/e2007-00062-4

THE EUROPEAN PHYSICAL JOURNAL D

Catalyst poisoning in the conversion of CO and N_2O to CO_2 and N_2 on Pt_4^- in the gas phase

C.-K. Siu[1,2], S.J. Reitmeier[1], I. Balteanu[1], V.E. Bondybey[1], and M.K. Beyer[1,3,a]

[1] Department Chemie, Lehrstuhl 2 für Physikalische Chemie, Technische Universität München, Lichtenbergstrasse 4, 85747 Garching, Germany
[2] Department of Chemistry and Centre for Research in Mass Spectrometry, York University, 4700 Keele Street, Toronto, Ontario, Canada M3J1P3
[3] Institut für Chemie, Sekr. C4, Technische Universität Berlin, Strasse des 17 Juni 135, 10623 Berlin, Germany

Received 23 July 2006 / Received in final form 13 October 2006

Abstract. Pt_4^- catalyses the conversion of CO and N_2O to CO_2 and N_2 in the gas phase, as observed by Fourier transform ion cyclotron (FT-ICR) mass spectrometry. The partial pressures of CO and N_2O determine the extent of poisoning and the turnover numbers that can be achieved. The catalytic conversion terminates as soon as two CO are adsorbed on the cluster. With N_2O, the reactivity of $Pt_4O_2^-$ and $Pt_4O_3^-$ is reduced to 41% and 34% compared to Pt_4O^-, respectively, and with $Pt_4O_4^-$ this value is reduced to 1%. In contrast, Pt_4^+ shows no apparent catalytic activity. Density functional theory calculations of $Pt_4^{+/-}$ with CO and N_2O adsorbates reveal significantly different stabilities of the reaction intermediates for the different charge states.

PACS. 31.15.Ew Density-functional theory – 33.15.Ta Mass spectra – 36.40.Jn Reactivity of clusters

1 Introduction

The oxidation of CO to CO_2 with N_2O catalyzed by Fe^+ in an FT-ICR mass spectrometer, as observed by Kappes and Staley [1], is the first example of a full catalytic cycle in the gas phase. Since then, a wide variety of metal ions and ionic clusters have been found to exhibit similar catalytic activities [2]. These gas phase models of the ideal single-site catalyst have recently been reviewed by Bohme and Schwarz [3]. Platinum is a key component in industrial catalysts, ranging from automotive catalytic converters to hydrogenation catalysts [4]. In the gas phase, already the monatomic Pt^+ catalyses the oxidation of CO. N_2O oxidizes the metal center in two steps to PtO^+ and PtO_2^+, and both species are reduced by CO to form CO_2 [5]. Ervin and coworkers observed the individual steps of full catalytic cycles of the same reaction on anionic platinum clusters with three to six atoms in a guided ion beam apparatus [6]. Inherent to the guided ion beam technique, however, the same cluster could not be used again in the reaction. Using an FT-ICR mass spectrometer, we were able to identify Pt_7^+, Pt_7O^+, $Pt_7O_2^+$, and Pt_7CO^+ as active species in the complete catalytic cycle, with a turnover number of 515 [7]. Adsorption of more than two CO molecules, however, completely quenched the catalytic activity, so that elevated CO partial pressures reduced the turnover numbers. No such effect was observed with elevated N_2O pressures on Pt_7^+. Here we investigate the catalytic activity of Pt_4^+ and Pt_4^-, which are known as the least reactive cationic and most reactive anionic platinum clusters, respectively [8,9].

2 Experimental and computational details

Isotopically enriched platinum (97.28% ^{195}Pt, Oak Ridge National Laboratories) was used to investigate the reactions of platinum clusters $^{195}Pt_4^{+/-}$ with CO and N_2O under binary collision conditions in a Fourier transform ion cyclotron resonance (FT-ICR) mass spectrometer. The experimental procedure was described in details previously [7,10]. The platinum ions are produced by pulsed laser vaporisation [11] of a rotating platinum disk and transferred to the ICR cell with a system of electrostatic lenses. To study catalytic cycles, CO and N_2O were introduced simultaneously into the ICR cell via two needle valves. In the 9:2 mixture, $p(CO) = 9.0 \times 10^{-8}$ mbar and $p(N_2O) = 2.1 \times 10^{-8}$ mbar. In the 1:20 mixture, $p(CO) = 5.2 \times 10^{-9}$ mbar and $p(N_2O) = 1.1 \times 10^{-7}$ mbar. The trapping voltage of ±2.5 V yields an upper limit of the collision energy in the center-of-mass frame of the collision partners of 0.1 eV. Mass spectra were taken after different reaction delays. The experimental

---

[a] e-mail: `martin.beyer@mail.chem.tu-berlin.de`

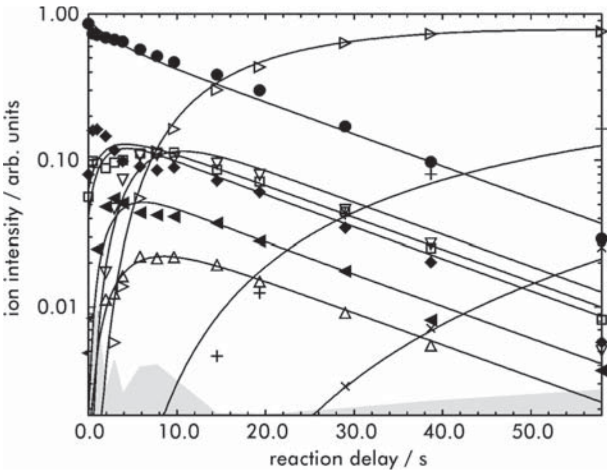

Fig. 1. Time-intensity profile of the reaction of Pt_4^- (●) with a 5:3 mixture of CO and N_2O. In collisions with N_2O, Pt_4O^- (□) and $Pt_4O_2^-$ (△) are formed. Sequential CO adsorption leads to $Pt_4(CO)_n^-$, with $n = 1$ (♦), $n = 2$ (◀), $n = 3$ (▽), $n = 4$ (▷), $n = 5$ (+) and $n = 6$ (×). The solid lines result from a fit of the experimental data to pseudo-first order kinetics employing a genetic algorithm, in which all chemically possible reaction pathways were allowed. The grey shaded area denotes the noise level.

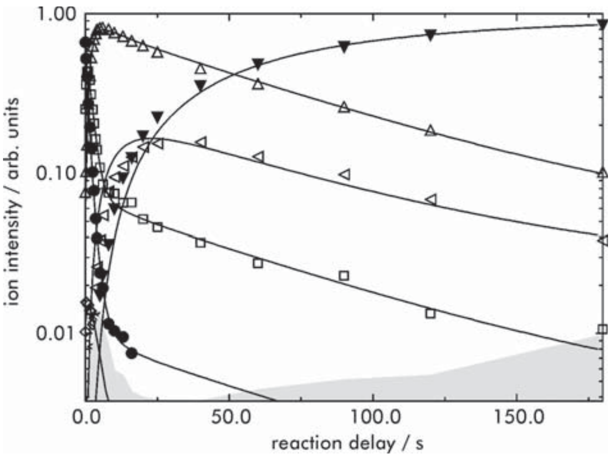

Fig. 2. Time-intensity profile of the reaction of Pt_4^- (●) with a 1:20 mixture of CO and N_2O. In collisions with CO, Pt_4CO^- (◊) is formed to a small extent. Sequential decomposition of N_2O leads to $Pt_4O_n^-$, with $n = 1$ (□), $n = 2$ (△), $n = 3$ (◁), and $n = 4$ (▼). The solid lines result from a fit of the experimental data to pseudo-first order kinetics employing a genetic algorithm, in which all chemically possible reaction pathways were allowed. The grey shaded area denotes the noise level.

results were fitted with a genetic algorithm [12] to pseudo-first order kinetics. Density functional calculations were performed with the Vienna Ab Initio Simulation Package (VASP) [13], employing the revised Perdew-Burke-Ernzerhof functional [14] together with plane-wave basis sets with a cut-off value of 282.84 eV. All structures were fully optimized. The reported energies are equilibrium energies without further corrections.

3 Results and discussion

Pt_4^+ is unreactive against N_2O [9], and adsorbs a first CO molecule very slowly. No evidence for catalytic activity was found: the intensity of the Pt_4CO^+ product is slowly increasing with time. In contrast, Pt_4^- was found to be the most reactive anionic cluster in the reaction with N_2O, forming the oxide Pt_4O^- [9]. Efficient catalytic conversion of CO to CO_2 is observed when CO and N_2O are present at constant partial pressures in the ICR cell. Figure 1 shows the results with a 9:2 mixture of CO and N_2O. In the first 5 s, the temperature, more precisely the internal energy distribution, of the clusters has not yet reached a stationary state, and the measured intensities deviate significantly from the fit. The long-term behavior, however, is very well reproduced by the fit.

In the 9:2 mixture, Pt_4^- is oxidized twice to Pt_4O^- and $Pt_4O_2^-$. Both species readily lose an O atom in collisions with CO, forming the CO_2 product of the catalytic cycle. With CO, Pt_4^- slowly forms the Pt_4CO^- complex, which is converted back to Pt_4^- at a similarly slow rate in collisions with N_2O. Pt_4CO^- is an active species in the catalytic cycle. As soon as a second CO is adsorbed, however, the $Pt_4(CO)_n^-$, $n \geqslant 2$, is no longer able to activate N_2O. Sequential addition of CO is the only reaction observed for those species. The genetic algorithm actively optimizes the rate constants of the reaction

$$Pt_4(CO)_n^- + N_2O \rightarrow Pt_4(CO)_{n-1}^- + CO_2 + N_2$$

to exactly 0.000 s^{-1} for $n \geqslant 2$, while it is 0.054 s^{-1} for $n = 1$.

With the 1:20 mixture of CO and N_2O used in the experiment of Figure 2, Pt_4^- is oxidized four times in the reaction

$$Pt_4O_n^- + N_2O \rightarrow Pt_4O_{n+1}^- + N_2.$$

The backward reaction with CO to form CO_2,

$$Pt_4O_n^- + CO \rightarrow Pt_4O_{n-1}^- + CO_2,$$

is very efficient for $n = 1$. Its rate constant is reduced to 41% and 34% of the initial value for $n = 2$ and $n = 3$, respectively. With 1% for $n = 4$, the reaction has more or less ceased.

The experimental results show an abrupt poisoning of the Pt_4^- catalyst upon adsorption of a second CO molecule, similar to Pt_7^+ [7]. Pt_4^-, however, may also be poisoned if the N_2O partial pressure is excessive. In this case, the poisoning is more gradual. Even in saturation, assuming that each Pt atom binds one O atom in $Pt_4O_4^-$, CO still seems to be able to abstract an O atom to form CO_2, albeit very slowly. Obviously, N_2O activation is more easily poisoned than CO adsorption. Figure 3 summarizes the complete catalytic cycle with the five active species and the routes to substrate poisoning both with CO and O. The absolute rate constants k_{abs} of the individual reactions are given in Table 1, and compared with the collision rate k_{SCC} estimated with the surface charge capture model [15]. Comparison of the absolute rates shows that the reactions are more efficient in the 1:20 mixture. This

Table 1. Absolute experimental rate constants of the reactions displayed in Figure 3, extracted from the fits in Figures 1 and 2. The collision rate k_{SCC} was calculated with the surface charge capture model [15] and amounts to 10.75×10^{-10} cm^3 s^{-1} for N_2O and 12.44×10^{-10} cm^3 s^{-1} for CO.

	$p(CO):p(N_2O) = 9:2$		$p(CO):p(N_2O) = 1:20$	
Reaction	$k_{abs}/10^{-10}$ cm^{3}s^{-1}	k_{abs}/k_{SCC}	$k_{abs}/10^{-10}$ cm^{3}s^{-1}	k_{abs}/k_{SCC}
$Pt_4CO^- + N_2O \rightarrow Pt_4^- + CO_2 + N_2$	1.07	0.099	1.13	0.105
$Pt_4^- + N_2O \rightarrow Pt_4O^- + N_2$	1.70	0.158	3.89	0.362
$Pt_4O^- + N_2O \rightarrow Pt_4O_2^- + N_2$	1.36	0.126	2.82	0.263
$Pt_4O_2^- + N_2O \rightarrow Pt_4O_3^- + N_2$			0.11	0.010
$Pt_4O_3^- + N_2O \rightarrow Pt_4O_4^- + N_2$			0.23	0.022
$Pt_4O_4^- + CO \rightarrow Pt_4O_3^- + CO_2$			0.13	0.010
$Pt_4O_3^- + CO \rightarrow Pt_4O_2^- + CO_2$			3.85	0.309
$Pt_4O_2^- + CO \rightarrow Pt_4O^- + CO_2$	1.65	0.132	4.65	0.374
$Pt_4O^- + CO \rightarrow Pt_4^- + CO_2$	1.75	0.140	11.25	0.904
$Pt_4^- + CO \rightarrow Pt_4CO^-$	0.37	0.029	1.28	0.103
$Pt_4CO^- + CO \rightarrow Pt_4(CO)_2^-$	1.55	0.125		
$Pt_4(CO)_2^- + CO \rightarrow Pt_4(CO)_3^-$	3.49	0.280		
$Pt_4(CO)_3^- + CO \rightarrow Pt_4(CO)_4^-$	1.36	0.109		
$Pt_4(CO)_4^- + CO \rightarrow Pt_4(CO)_5^-$	0.02	0.002		
$Pt_4(CO)_5^- + CO \rightarrow Pt_4(CO)_6^-$	0.03	0.003		

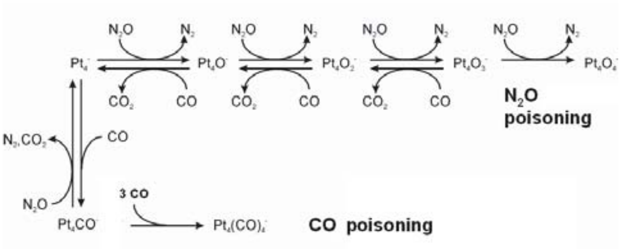

Fig. 3. Complete catalytic cycle of the oxidation of CO with N_2O to CO_2 and N_2 on Pt_4^-. The catalytic activity ceases, i.e. the catalyst is poisoned, when $Pt_4O_4^-$ or $Pt_4(CO)_4^-$ are reached.

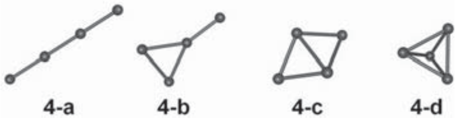

Fig. 4. Four different structural types considered in the calculations of $Pt_4^{+/-}$.

is in line with the internal energy distribution in the stationary state. In the 9:2 mixture, more CO_2 is formed, and the heat of formation partly stays in the clusters. This enhances the probability for back-dissociation of the collision complex, before new chemical bonds can be formed.

In order to rationalize the different behavior of Pt_4^+ and Pt_4^-, we investigated the stability of the bare clusters and characteristic reaction intermediates of the initial reaction with CO and N_2O. Figure 4 illustrates the investigated geometries of bare clusters. Table 2 lists the relative energies and bond distances found in the optimized structures, together with the magnetic moment. Pt_4^+ is definitely a regular tetrahedron, structure 4-d, while in the case of Pt_4^-, the nearly planar structure 4-c and the planar structure 4-b are isoenergetic. CO is coordinated in an atop position, to individual platinum atoms. The binding energy is 2.2 eV in Pt_4CO^+ and 3.1 eV in Pt_4CO^-. The anionic platinum tetramer binds CO 0.9 eV more strongly than the corresponding cationic species. Together with the limited degrees of freedom in such a small system, this explains the different reactivity of the bare clusters against CO. Experimental results for the binding energies of CO to platinum cluster anions lie in the range of 2.3–2.6 eV [16], not too far from the calculated value.

With N_2O, the potential energy surface is more complicated. First, N_2O adsorbs in an atop position, forming a Pt-N bond in $Pt_4(N_2O)^{+/-}$. The binding energy is 1.0 eV for the cation and 1.4 eV for the anion. The difference gets more pronounced for the insertion compound $OPt_4N_2^{+/-}$, which lies 2.5 eV below $Pt_4^+ + N_2O$ and 4.1 eV below $Pt_4^- + N_2O$. The overall exothermicity of the reaction

$$Pt_4^{+/-} + N_2O \rightarrow Pt_4O^{+/-} + N_2$$

is 1.3 eV for the cation and 2.6 eV for the anion. Due to the inherent limitation of the computational approach — the size of the basis set and the absence of thermal corrections — these absolute values have to be treated with care. A complete examination of the potential energy surface should also include transition states. However, the results unambiguously show that Pt_4^- exhibits stronger bonds than Pt_4^+. Given the strong spin-orbit coupling in third-row transition metals [17], spin crossing is efficient, which rules out spin problems as an alternative explanation. This indicates that the overall thermochemistry of the reaction makes Pt_4^- much more reactive than Pt_4^+, in agreement with an earlier observation by Koszinowski et al. who showed that the low reactivity of Pt_4^+ against CH_4 has thermochemical reasons [18].

Table 2. Relative energies without zero-point correction of the four isomers shown in Figure 3 for the two studied charge states, cationic and anionic. Energies are given in eV relative to the most stable isomer. The range of Pt–Pt distances d(Pt–Pt) is given in Å, the magnetic moment μ_B in a.u. corresponds largely to the spin multiplicity.

	cationic Pt_4^+			anionic Pt_4^-		
Structure	ΔE in eV	d(Pt–Pt) in Å	μ_B	ΔE in eV	d(Pt–Pt) in Å	μ_B
4-a	2.35	2.30–2.32	1.10	0.73	2.36–2.39	3.11
4-b	1.37	2.34–2.50	3.00	**0.00**	2.37–2.52	1.03
4-c	0.70	2.50–2.62	3.00	**0.01**	2.54–2.55	3.00
4-d	**0.00**	2.57	2.86	0.56	2.57–2.69	5.00

4 Conclusions

Pt_4^- is a very active catalyst for the conversion of CO to CO_2 with N_2O, while Pt_4^+ reacts only with slow addition of CO. This difference is rationalized with density functional calculations, which show that both species have a different geometry, a near-planar anion and a tetrahedral cation. Pt_4^- forms significantly stronger bonds than Pt_4^+ with both reactants, indicating that the different behavior has thermochemical rather than mechanistic reasons. Catalyst poisoning is observed with both N_2O and CO. The catalytic activity ceases when either $Pt_4(CO)_2^-$ or $Pt_4O_4^-$ is reached in the process.

This work was supported by the Deutsche Forschungsgemeinschaft, the Fonds der Chemischen Industrie, the Alexander von Humboldt-Foundation (C.-K.S.) and the Heisenberg program of the Deutsche Forschungsgemeinschaft (M.K.B.).

References

1. M.M. Kappes, R.H. Staley, J. Am. Chem. Soc. **103**, 1286 (1981)
2. M. Andersson, A. Rosén, J. Chem. Phys. **117**, 7051 (2002); P. Schnabel, K.G. Weil, M.P. Irion, Angew. Chem. Int. Edit. **31**, 636 (1992); L.D. Socaciu, J. Hagen, T.M. Bernhardt, L. Woste, U. Heiz, H. Hakkinen, U. Landman, J. Am. Chem. Soc. **125**, 10437 (2003)
3. D.K. Bohme, H. Schwarz, Angew. Chem. Int. Edit. **44**, 2336 (2005)
4. M. Kraus, in *Handbook of Heterogeneous Catalysis*, edited by G. Ertl, H. Knözinger, J. Weitkamp (VCH, Weinheim, 1997), Vol. 3, p. 1051; H. Arnold, F. Döbert, J. Gaube, in *Handbook of Heterogeneous Catalysis*, edited by G. Ertl, H. Knözinger, J. Weitkamp (VCH, Weinheim, 1997), Vol. 5, p. 2165; F.J. Janssen, in *Handbook of Heterogeneous Catalysis*, edited by G. Ertl, H. Knözinger, J. Weitkamp (VCH, Weinheim, 1997), Vol. 4, p. 2165
5. M. Brönstrup, D. Schröder, I. Kretzschmar, H. Schwarz, J.N. Harvey, J. Am. Chem. Soc. **123**, 142 (2001)
6. Y. Shi, K.M. Ervin, J. Chem. Phys. **108**, 1757 (1998)
7. O.P. Balaj, I. Balteanu, T.T.J. Roßteuscher, M.K. Beyer, V.E. Bondybey, Angew. Chem. **116**, 6681 (2004)
8. U. Achatz, C. Berg, S. Joos, B.S. Fox, M.K. Beyer, G. Niedner-Schatteburg, V.E. Bondybey, Chem. Phys. Lett. **320**, 53 (2000)
9. I. Balteanu, O.P. Balaj, M.K. Beyer, V.E. Bondybey, Phys. Chem. Chem. Phys. **6**, 2910 (2004)
10. C. Berg, T. Schindler, G. Niedner-Schatteburg, V.E. Bondybey, J. Chem. Phys. **102**, 4870 (1995)
11. S. Maruyama, L.R. Anderson, R.E. Smalley, Rev. Sci. Instrum. **61**, 3686 (1990); V.E. Bondybey, J.H. English, J. Chem. Phys. **74**, 6978 (1981); T.G. Dietz, M.A. Duncan, D.E. Powers, R.E. Smalley, J. Chem. Phys. **74**, 6511 (1981)
12. D. Goldberg, *Genetic algorithms in search, optimization, and machine learning* (Addison-Wesley, Reading, Massachusetts, 1989)
13. G. Kresse, J. Furthmuller, Phys. Rev. B **54**, 11169 (1996)
14. J.P. Perdew, K. Burke, M. Ernzerhof, Phys. Rev. Lett. **77**, 3865 (1996); Y. Zhang, W. Yang, Phys. Rev. Lett. **80**, 890 (1998); B. Hammer, L.B. Hansen, J.K. Nørskov, Phys. Rev. B **59**, 7413 (1999)
15. G. Kummerlöwe, M.K. Beyer, Int. J. Mass Spectrom. **244**, 84 (2005)
16. A. Grushow, K.M. Ervin, J. Chem. Phys. **106**, 9580 (1997)
17. H. Schwarz, Angew. Chem. Int. Edit. **42**, 4442 (2003)
18. K. Koszinowski, D. Schröder, H. Schwarz, J. Phys. Chem. A **107**, 4999 (2003)